

## Sex-specific effects of CD248 on metabolism and the adipose tissue lipidome

Patrick, Kieran; Tian, Xiang; Cartwright, David; Heising, Silke; Glover, Matthew S.; Northall, Ellie N.; Cazares, Lisa; Hess, Sonja; Baker, David; Church, Christopher; Davies, Graeme; Lavery, Gareth; Naylor, Amy J.

DOI:

[10.1371/journal.pone.0284012](https://doi.org/10.1371/journal.pone.0284012)

License:

Creative Commons: Attribution (CC BY)

### Document Version

Publisher's PDF, also known as Version of record

### Citation for published version (Harvard):

Patrick, K, Tian, X, Cartwright, D, Heising, S, Glover, MS, Northall, EN, Cazares, L, Hess, S, Baker, D, Church, C, Davies, G, Lavery, G & Naylor, AJ 2023, 'Sex-specific effects of CD248 on metabolism and the adipose tissue lipidome', *PLoS ONE*, vol. 18, no. 4, e0284012. <https://doi.org/10.1371/journal.pone.0284012>

[Link to publication on Research at Birmingham portal](#)

### General rights

Unless a licence is specified above, all rights (including copyright and moral rights) in this document are retained by the authors and/or the copyright holders. The express permission of the copyright holder must be obtained for any use of this material other than for purposes permitted by law.

- Users may freely distribute the URL that is used to identify this publication.
- Users may download and/or print one copy of the publication from the University of Birmingham research portal for the purpose of private study or non-commercial research.
- User may use extracts from the document in line with the concept of 'fair dealing' under the Copyright, Designs and Patents Act 1988 (?)
- Users may not further distribute the material nor use it for the purposes of commercial gain.

Where a licence is displayed above, please note the terms and conditions of the licence govern your use of this document.

When citing, please reference the published version.

### Take down policy

While the University of Birmingham exercises care and attention in making items available there are rare occasions when an item has been uploaded in error or has been deemed to be commercially or otherwise sensitive.

If you believe that this is the case for this document, please contact [UBIRA@lists.bham.ac.uk](mailto:UBIRA@lists.bham.ac.uk) providing details and we will remove access to the work immediately and investigate.

## RESEARCH ARTICLE

# Sex-specific effects of CD248 on metabolism and the adipose tissue lipidome

Kieran Patrick<sup>1</sup>, Xiang Tian<sup>2</sup>, David Cartwright<sup>3</sup>, Silke Heising<sup>3</sup>, Matthew S. Glover<sup>2</sup>, Ellie N. Northall<sup>1</sup>, Lisa Cazares<sup>2</sup>, Sonja Hess<sup>2</sup>, David Baker<sup>4</sup>, Christopher Church<sup>4</sup>, Graeme Davies<sup>4</sup>, Gareth Lavery<sup>3</sup>, Amy J. Naylor<sup>1\*</sup>

**1** Institute of Inflammation and Ageing, University of Birmingham, Birmingham, United Kingdom, **2** Dynamic Omics, Centre for Genomics Research, Discovery Sciences, Biopharmaceuticals R&D, AstraZeneca, Gaithersburg, MD, United States of America, **3** Institute of Metabolism and Systems Research, University of Birmingham, Birmingham, United Kingdom, **4** BioPharmaceuticals R&D, Cardiovascular, Renal and Metabolism (CVRM), Cambridge, United Kingdom

\* [a.naylor@bham.ac.uk](mailto:a.naylor@bham.ac.uk)



## OPEN ACCESS

**Citation:** Patrick K, Tian X, Cartwright D, Heising S, Glover MS, Northall EN, et al. (2023) Sex-specific effects of CD248 on metabolism and the adipose tissue lipidome. PLoS ONE 18(4): e0284012. <https://doi.org/10.1371/journal.pone.0284012>

**Editor:** Josep A. Villena, Vall d'Hebron Institut de Recerca, SPAIN

**Received:** September 20, 2022

**Accepted:** March 22, 2023

**Published:** April 28, 2023

**Copyright:** © 2023 Patrick et al. This is an open access article distributed under the terms of the [Creative Commons Attribution License](https://creativecommons.org/licenses/by/4.0/), which permits unrestricted use, distribution, and reproduction in any medium, provided the original author and source are credited.

**Data Availability Statement:** All relevant data are within the paper and its [Supporting Information](#) files. Additional data for this study are publicly available from the MetaboLights repository (<https://www.ebi.ac.uk/metabolights/MTBLS6615>).

**Funding:** KP, AJN and GL received funding from AstraZeneca as part of a collaborative research grant. Co-authors from AstraZeneca (XT, MSG, LC, SH, DB, CC and GD) were involved in the study design, data collection and analysis, decision to publish and preparation of the manuscript. AJN

## Abstract

*Cd248* has recently been associated with adipose tissue physiology, demonstrated by reduced weight gain in high fat diet-fed mice with genetic deletion of *Cd248* relative to controls. Here we set out to determine the metabolic consequences of loss of *Cd248*. Strikingly, we find these to be sex specific; By subjecting *Cd248*<sup>-/-</sup> and *Cd248*<sup>+/+</sup> mice to a high fat diet and indirect calorimetry study, we identified that only male *Cd248*<sup>-/-</sup> mice show reduced weight gain compared to littermate control wildtype mice. In addition, male (but not female) mice showed a lower respiratory exchange ratio on both chow and high fat diets, indicating a predisposition to metabolise lipid. Lipidomic studies on specific fat depots found reduced triglyceride and diglyceride deposition in male *Cd248*<sup>-/-</sup> mice, and this was supported by reduced expression of lipogenic and adipogenic genes. Finally, metabolomic analysis of isolated, differentiated preadipocytes found alterations in metabolic pathways associated with lipid deposition in cells isolated from male, but not female, *Cd248*<sup>-/-</sup> mice. Overall, our results highlight the importance of sex controls in animal studies and point to a role for *Cd248* in sex- and depot-specific regulation of lipid metabolism.

## Introduction

Adipose tissue is a highly sexually dimorphic tissue across many species. Lipid accumulation within separate anatomical regions is often part of secondary sexual characteristics [1], for example, male mice have a larger gonadal fat pad than females [2]. The lipid storage capacity of the perirenal fat pad is limited in male mice, and this results in metabolic syndrome during obesity models [3]. In humans, females are predisposed to accumulate fat in the lower body whilst males tend to accumulate fat in the abdomen, and this is linked to metabolic disease where the relatively greater levels of visceral fat observed in males are linked to a greater risk of developing type 2 diabetes [4].

Understanding the mechanisms that underlie sex-specific differences in lipid deposition, and the extent to which lipid accumulation in specific depots impacts whole-body metabolic

also received funding from a Versus Arthritis Career Development Fellowship #21743.

**Competing interests:** I have read the journal's policy and the authors of this manuscript have the following competing interests: XT, MSG, LC, SH, DB, CC, GD are employees of AstraZeneca and may own stocks and/or restricted stocks. This does not alter our adherence to PLOS ONE policies on sharing data and materials.

activity, is a key area of investigation in the pursuit of developing treatments for metabolic disease. Sex differences in adipose tissue are driven in large part by differences in sex hormones [5, 6], and recently sex hormones have been shown to control the size of adipocyte progenitor pools [7]. Prior to sexual maturity, differential gene expression between sexes is driven by sex chromosome karyotype and developmental genes contributing to intrinsic sex differences and is independent of hormonal signals [1, 2, 8]. Thus, the effect of a particular gene's expression within adipose tissue in males and females can be affected by both hormonal and cell-intrinsic gene expression differences.

*Cd248* (Endosialin, TEM1) is a transmembrane glycoprotein that is expressed almost exclusively on mesenchymal stem cell (MSC) lineage cells including osteoblasts [9], fibroblasts [10], and adipocytes [11]. *Cd248* expression is high during development and is then downregulated in normal adult tissue. In the adult, increased expression has been associated with pathological tissue remodelling and it is seen particularly highly expressed in cancer associated fibroblasts [12], in fibrotic kidney disease [13], in inflammation associated with arthritis [14], and in atherosclerotic plaques [15]. Recently, *Cd248* has been associated with lipid accumulation and metabolism [11, 16]. Specifically, *Cd248*<sup>-/-</sup> mice are protected from obesity and glucose intolerance when fed a high fat diet [11] and the serum lipid profile of *Cd248*<sup>-/-</sup> mice on a high fat diet is altered [16], suggesting differences in lipid synthesis pathways. Here, we demonstrate that reduced weight gain in *Cd248*<sup>-/-</sup> mice on a high fat diet is, in fact, sex specific; with only males showing this phenotype. Additionally, we uncover depot-specific differences in fat pad lipid profiles, and site-specific alterations in gene expression.

## Materials and methods

### Chemicals and reagents

Isopropanol (Honeywell, catalog no. 34965-4X4L), Ethyl acetate (Millipore Sigma, catalog no. 103649), Methanol (Avantor, catalog no. 9830-3), Toluene (Sigma-Aldrich, catalog no. 650579), Acetonitrile (Fisher Chemical, catalog no. A955-4), Formic acid (Fisher Chemical, catalog no. A117-50) and Ammonium formate (Sigma-Aldrich, catalog no. 70221-100G-F).

### Mice

All animal experiments were performed in accordance with U.K. laws [Animal (Scientific Procedures) Act 1986] and with the approval of the Local Ethics Committees at the University of Birmingham. Every effort has been made to present all data in accordance with the ARRIVE guidelines (NC3Rs) [17]. The generation and genotyping of *Cd248*<sup>-/-</sup> mice have been described previously [18]. Mice were subsequently backcrossed for >10 generations onto a C57BL/6J background and confirmed by SNP analysis (Transnetyx Inc, Cordova). Genotyping was carried by Transnetyx Inc, Cordova. Mice were maintained on a 12 h light/dark cycle at 21°C with *ad libitum* access to food and water. All mice were generated from CD248<sup>+/-</sup> x CD248<sup>+/-</sup> pairs. Mice were fed either a standard chow diet containing 10% kcal from fat, high in fibre containing complex carbohydrates (Special Diets Services U.K. RM3 (P) 801700), or a high fat diet containing 60% kcal from fat (Research Diets Inc, Rodent Diet With 60 kcal% Fat RD12492).

### High fat diet indirect calorimetry, weight gain and glucose tolerance study

Cohort breeding from *Cd248* heterozygote (*Cd248*<sup>+/-</sup>) male and female pairs resulted in 7x *Cd248*<sup>+/+</sup> male, 10x *Cd248*<sup>-/-</sup> male, 6x *Cd248*<sup>+/-</sup> female and 7x *Cd248*<sup>-/-</sup> female mice. Results from all animals are included in the results (heterozygote offspring were not included in any

experiments). From weaning (week 4) until week 8 mice were fed standard chow. From 8 weeks of age mice were fed high fat diet for a further 16 weeks (until 23 weeks of age). At the end of the experiment, mice were anaesthetised with isoflurane and a bolus serum blood sample obtained through cardiac puncture. Fat pads (inguinal, scapular, perirenal, gonadal) were collected, snap frozen in liquid nitrogen and stored at  $-80^{\circ}\text{C}$ .

### CL316,243 injection study and primary cell isolation (preadipocyte extraction)

6–12 week old chow-fed mice were used. 15x *Cd248*<sup>+/+</sup> male, 14x *Cd248*<sup>-/-</sup> male, 7x *Cd248*<sup>+/+</sup> female, 7x *Cd248*<sup>-/-</sup> female. Results from all animals are included in the results.

### Indirect calorimetry

Indirect calorimetry to assess energy metabolism was performed using the PhenoMaster System (TSE systems, Bad Homburg, Germany). Between 6–8 weeks of age, baseline energy metabolism on chow diet was assessed. Subsequently, energy metabolism was assessed after 6 and 12 weeks of high fat diet feeding.

Oxygen consumption rate ( $\text{VO}_2$ ), carbon dioxide production ( $\text{VCO}_2$ ), heat production, respiratory exchange ratio (RER), and food and drink intake were each measured (method as previously described [19]) over a 72-hour time frame with only the last 48 hours included in the analysis. Briefly, mice were placed into the PhenoMaster System in litter-mate groups for 24 hours to acclimatise to the altered environment. Subsequently the mice were separated and housed individually for 72 hours to enable collection of accurate individual recordings, with the first 24 hours discounted whilst the mice acclimatized to single housing. At the end of each period of indirect calorimetry recording, mice were returned to their cage groups.

In CL316,243 stimulation studies, mice were placed into the PhenoMaster system in cage groups for 24 hours to acclimatise (as above) and subsequently single-housed for 3 hours to attain a baseline measurement. CL316,243 (1 mg/Kg body weight, PBS solution, intraperitoneal injection) was then administered, followed by a further 3 hours of measurement, after which mice were returned to their cage groups.

### Glucose tolerance test

Mice were fasted for a 6-hour period and a small incision made in the distal tail vein, from which baseline (and all subsequent) blood glucose measurements were taken. Mice were then given a glucose bolus (2 g/Kg body weight, water solution, intraperitoneal injection) and blood glucose measurements were taken using a Contour XT glucometer (Bayer) at 15, 30, 60 and 120 min.

### Preadipocyte extraction and cell culture

Preadipocytes were extracted from the stromal vascular fraction (SVF) of inguinal fat pads. Briefly, mice aged 8–12 weeks old on chow diet were culled by cervical dislocation and fat pads dissected. Fat pads were finely minced, and collagenase digested ( $37^{\circ}\text{C}$ , 1 hour with constant agitation). The resulting cell suspension was filtered to remove debris (70  $\mu\text{m}$  pore size) and pelleted (300g, 3 min.) to separate mature adipocytes (which remain in the supernatant) from pelleted preadipocytes. Mature adipocytes and supernatant were discarded, whilst the SVF was resuspended in DMEM/F12 (Gibco, 10% FCS, 2 mM L-GLN, 100 U/ml Pen-Strep) and plated onto tissue culture plastic. Preadipocytes were used in experiments at passage 0.

### Adipocyte differentiation protocol

Passage 0 preadipocytes were cultured to 80–100% confluency in DMEM/F12. Subsequently induction media was applied for 2 days and afterwards maintenance media applied for 5 days. Induction media: Insulin (bovine) 1 µg/ml Sigma (I6634), dexamethasone 0.25 µg/ml Sigma (D4902), IBMX 30 µg/ml Sigma (I5879), rosiglitazone 1 µM (Cayman #71740). Maintenance media: Insulin (bovine) 1 µg/ml Sigma (I6634). At the end of the protocol cells were used for RNA or metabolite extraction.

### RNA extraction and cDNA synthesis

Cells or tissues were suspended in RLT buffer containing 1% w/v β-mercaptoethanol. Cells were lysed by agitation and repeated aspiration; tissue was lysed using the TissueLyser Sample Disrupter system (QIAGEN). Lysates were homogenised by passing through QIAshredder (QIAGEN) with centrifugation (2 min, 18,000 rcf). Samples were then taken through RNA Mini Kit protocol (QIAGEN) as per the manufacturer's instructions. DNase digestion was performed on column. RNA concentration was determined by nanodrop (ThermoFisher). cDNA synthesis was performed on 500 ng of RNA in a 20 µL reaction using the High-Capacity cDNA Reverse Transcription Kit (Applied Biosystems) as per the manufacturer's instructions.

### Gene expression analysis

Preamplification of cDNA was performed: 8 µL total reaction volume comprising 4 µL Taqman Preamp Mastermix, 2 µL Custom Preamp pool of primers (ThermoFisher, Waltham, USA) and 2 µL cDNA. Thermocycler protocol: 95°C for 10 mins, 14 cycles of 95°C for 15 seconds and 60°C for 4 mins. Samples were diluted 1:10 with nuclease free water and 3 µL sample was added into an OpenArray 384 well sample plate with 3 µL OpenArray Real Time PCR Master Mix. Samples were loaded by OpenArray Accufill System onto Custom Taqman OpenArray plates (ThermoFisher, Waltham, USA) containing 56 Taqman gene expression assays. Plates were sealed according to the manufacturer's instructions and run on a QuantStudio 12K Flex Real-Time PCR System (ThermoFisher, Waltham, USA). Gene expression results were normalised to the reference genes PPIA, RPLP0, B2M and HPRT. Differentially expressed genes were defined as having a > 1.5-fold change from control and  $p < 0.05$  (t-test). Details of the targets within the panel are in [S5 Table](#).

### Luminex cytokine & chemokine 36-Plex mouse ProcartaPlex™ panel 1A

Frozen serum samples from high fat diet mice were thawed on ice and run through the Luminex assay according to the manufacturer's instructions. Briefly, samples were diluted according to the kit supplied protocol and added to 96 well plate alongside protein standards. Primary antibody conjugated magnetic beads were incubated in the samples for 2 hours. The beads were then washed. Next detection antibodies were added and incubated for 30 min. Beads were washed and streptavidin-PE was added and incubated for 30 min. Beads were washed and resuspended in reading buffer. Data were acquired on a Luminex system. Details of the targets within the panel are in [S5 Table](#).

### Lipid extraction adipose tissue

Extractions were performed using the following extraction solvent mixture IPA:H<sub>2</sub>O:EtOAc (30:10:60, v:v:v). 10 mg samples of adipose tissue were collected in 2.0 mL snap-top microcentrifuge tubes containing four 2.8 mm ceramic beads (VWR 215913). Samples were extracted in 1:10 volume of extraction solvent (10 mg tissue: 100 µL solvent mixture). Samples were

homogenised with Tissue-Lyser (QIAGEN) for 2 min. at 30 Hz, then centrifuged to separate the organic phase from cellular debris (15 min. 18,000 g, 20°C). 10 µL of the organic upper phase were transferred to fresh microcentrifuge tube. Samples were then dried in a SpeedVac (Thermo) without heat and stored at -80°C.

Lipids were reconstituted in 400 µL MeOH:toluene (90:10 v:v) with 0.5 µg/ml Equisplash (Avanti) as internal standard, mixed for 1 min. at 1500 rpm (Eppendorf ThermoMixer C) followed by a sonication for 2 min. Samples were mixed for another 1 min. at 1500 rpm before centrifugation for 5 min. at 16,000 g, 20°C. 50 µL of the supernatant from each sample were transferred to glass HPLC vials and 5 µL of each individual sample were combined to make the pooled QC sample [20]. Samples were randomized before analysing by LC-MS, with a QC run after every 10 study samples.

### Sample extraction of differentiated adipocytes for metabolomics

Extractions were performed using the solvent mixture 50% ACN, 50% H<sub>2</sub>O, 0.1% formic acid, and a 1µM isotopic labelled amino acid mixture as internal standards (Cambridge Isotope Laboratories Inc. MA, USA). Confluent wells of cells were aspirated completely of media and washed in ice cold PBS. Plates were placed onto dry ice and 1ml of extraction solvent was added to each well. Next the plates were incubated at -80°C for 10 min. Cells were thawed, scraped, and collected into snap-top microcentrifuge tubes, vortexed, then centrifuged at 16,000g at 4°C. 900 µL of supernatant was collected into fresh snap-top microcentrifuge tubes and evaporated to dryness in a Speedvac.

Metabolites were reconstituted in 60 µL ACN:H<sub>2</sub>O (3:1 v:v), then mixed for 1 min. at 1500 rpm (Eppendorf ThermoMixer C) followed by sonication for 2 min. Samples were mixed for another 1 min. at 1500 rpm before centrifugation (5 minutes at 16,000 g, 20°C). 50 µL supernatant from each sample was transferred to a glass HPLC vial (Waters) and analysed by LC-MS. 5 µL of each individual sample were combined to make a pooled QC. Samples were randomized before analysis by LC-MS with a QC run after every 6 study samples.

### LC-MS methods for lipidomics

LC-MS was performed on a Vanquish UHPLC (Thermo Scientific) coupled with Thermo Scientific Orbitrap ID-X Tribrid Mass Spectrometer. RP-LC was performed on a Vanquish UHPLC (Thermo Scientific), using a Waters ACQUITY UPLC CSH C18 column (1.7 µm, 2.1 mm × 100 mm, 130 Å) (P/N-186005297) with a sample injection volume of 1 µL. Mobile phase A consisted of 40% H<sub>2</sub>O and 60% ACN with 0.1% formic acid and 10 mM ammonium formate and mobile phase B was formed from 10% ACN and 90% IPA with 0.1% formic acid and 10 mM ammonium formate delivered at a constant flow rate of 0.6 mL/min. The gradient began with 15% mobile phase B and linearly increased to 30% from 0 to 2 min., then to 48% from 2 to 2.5 min., followed by a continuous increase to 82% from 2.5 to 11 min., finally rising to 99% from 11 to 11.5. After maintaining mobile phase B at 99% for 0.5 min. the percentage was reduced to 15% from 12 to 12.1 min. To re-equilibrate the column, 15% mobile phase B was used from 12.1 to 15 min. The temperature of the column oven was maintained at 65°C.

Mass spectrometry was performed on a Thermo Scientific Orbitrap ID-X Tribrid Mass Spectrometer, equipped with the EASY-IC internal calibration source, a divert/inject valve, and the Thermo Scientific OptaMax NG API source. MS1 analyses were conducted in positive ion mode using the following parameters (Voltage: 3500V positive ESI, Sheath gas: 50, Aux gas: 10, Sweep gas: 1, Ion transfer tube: 325°C, Vaporizer: 300°C, Resolution: 60k, Scan range: 60–900 *m/z*, AGC target: standard, microscans: 1). MS2 spectra of the pooled sample were acquired by AcquireX DeepScan iterative data-dependent acquisition workflow

(ThermoFisher) method with the following parameters (Quad isolation: 1 m/z, Resolution: 7.5k, Scan Range: 200–1200, AGC Target: Standard, microscans: 3).

### LC and MS methods for metabolomics

LC-MS was performed on a Vanquish UHPLC (Thermo Scientific) coupled with Thermo Scientific Orbitrap ID-X Tribrid Mass Spectrometer. HILIC-LC was performed on an Vanquish UHPLC (Thermo Scientific), using a Waters ACQUITY UPLC BEH Amide HILIC column (1.7  $\mu\text{m}$ , 2.1 mm  $\times$  150 mm, 130  $\text{\AA}$ ) (P/N– 186004802) with a sample injection volume of 1  $\mu\text{L}$ . The mobile phase A consisted of 100%  $\text{H}_2\text{O}$  with 0.125% formic acid and 10 mM ammonium formate) and mobile phase B was 95% ACN and 5%  $\text{H}_2\text{O}$  with 0.125% formic acid and 10 mM ammonium formate delivered at a constant flow rate of 0.4 mL/min. The gradient began with 100% mobile phase B for 2 mins and linearly decreased to 70% from 2 to 7.7 min. Then, dropped to 40% from 7.7 to 9.5 mins. After that, it continuously decreased to 30% from 9.5 to 10.25 min, then increased to 100% B from 10.25 to 12.75. To re-equilibrate the column, 100% mobile phase B was maintained from 12.75 to 16.75 min. The temperature of the column oven was set at 45°C.

Mass spectrometry was performed on a Thermo Scientific Orbitrap ID-X Tribrid Mass Spectrometer, equipped with the EASY-IC internal calibration source, a divert/inject valve, and the Thermo Scientific OptaMax NG API source. MS1 analyses were conducted using a polarity switching approach, where the Orbitrap ID-X MS was operated by alternating between positive and negative ESI modes using the following parameters (Voltage: 3500V positive ESI and 3000V negative ESI, Sheath gas: 50, Aux gas: 10, Sweep gas: 1, Ion transfer tube: 325°C, Vaporizer: 300°C, Resolution: 30k, Scan range: 60–900 m/z, AGC target: standard, Microscans: 1). MS2 spectra of the pooled sample were acquired by ddMS2 (deep scan) method with the following parameters (Quad isolation: 1 m/z, Resolution: 7.5k, Scan Range: 60–900, AGC Target: Standard, Microscans: 1).

### Data and statistical analysis

Lipidomics and metabolomics data analysis, including peak picking, alignment, smoothing, and annotation was performed using MSDial software. Feature annotation followed the Metabolomics Standards Initiative (MSI) levels [21]. The lipidomics data were normalized to the internal standard, EquiSPLASH (Avanti, Birmingham, AL, USA, SKU: 330731). The metabolomics data were normalized to total ion current (TIC). To remove the background noise, S/N threshold was set to 3. In addition, the lipids, or metabolites with relative standard deviation (RSD) higher than 30% in the pooled QC samples were also removed. The data were analysed in R using both in-house and MetaboAnalyst scripts, followed by analysis in GraphPad Prism software. Significance was calculated either by t-test when only one comparison was made, or by ANOVA where multiple comparisons were made. For gene expression data, differences were considered significant if t-test  $\leq 0.05$  along with fold change  $\geq 1.5$ . In the case of the indirect calorimetry data, where ANCOVA analysis was required to determine if the body weight covariable was determining RER, this was carried out using SPSS software ANCOVA tool. Data are presented as either  $\pm$  standard deviation (weight gain, food intake, average RER, gene expression) or  $\pm$  standard error of the mean (CL316,243 response, glucose tolerance test). Metabolite identifications were made according to the recommendations contained in the Metabolomics Society Initiative (MSI) as defined by Sumner et al (2007)[21]. All metabolomics data has been uploaded to the Metabolights repository, ID MTBLS6615:

<https://www.ebi.ac.uk/metabolights/MTBLS6615/descriptors>.

## Results

To determine if genetic deletion of *Cd248* confers protection against adiposity via changes to energy metabolism, mice were subjected to a high fat diet and weighed weekly for 16 weeks in parallel with a series of indirect calorimetry measurements. A sex-specific difference in weight gain was observed: Male *Cd248*<sup>-/-</sup> mice gained significantly less weight compared to littermate controls, whilst female *Cd248*<sup>-/-</sup> mice showed equal weight gain to littermate controls (Fig 1A & 1B). No differences in food consumption were detected either on chow or on high fat diet for either sex regardless of genotype (Fig 1C - 1F). To detect whether alterations in energy metabolism and/or fuel utilisation between *Cd248*<sup>-/-</sup> mice and littermate controls was the cause of the reduced weight gain phenotype, indirect calorimetry data was analysed for significance by ANCOVA. We found sex-specific differences in RER: male *Cd248*<sup>-/-</sup> mice showed significantly lower RER during the night period, both at baseline on chow diet and at 12 weeks of

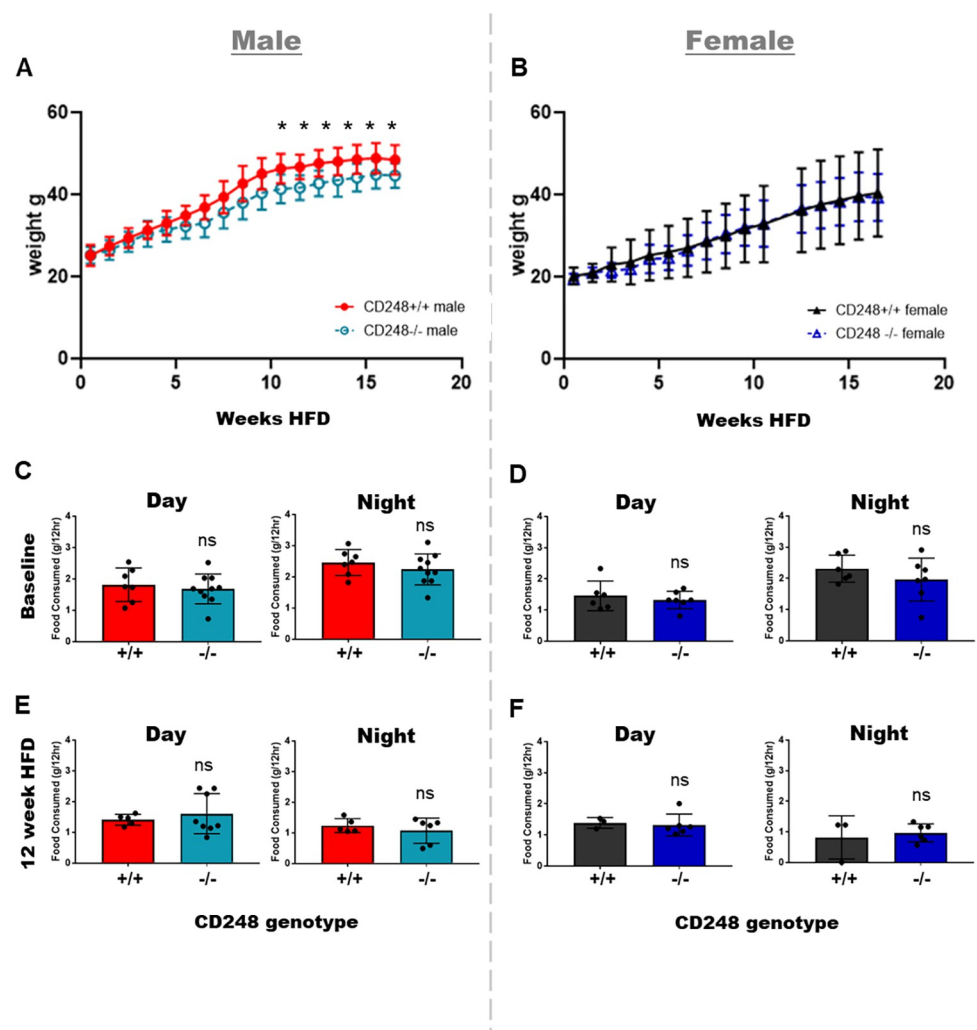


**Fig 1.** Weight gain  $\pm$ SD over 16 weeks of high fat diet in (A) males and (B) females. Food intake  $\pm$ SD at baseline (C) day and (D) night. Food intake over 12 hours after 12 weeks of high fat diet during the (E) day and (F) night. Body weight data over time were analysed for significant differences by t-test. Food intake was analysed by t-test. In all graphs: *Cd248*<sup>+/+</sup> males (red), *Cd248*<sup>-/-</sup> males (cyan), *Cd248*<sup>+/+</sup> females (black), *Cd248*<sup>-/-</sup> females (blue). Significant \*  $p \leq 0.05$ .

<https://doi.org/10.1371/journal.pone.0284012.g001>



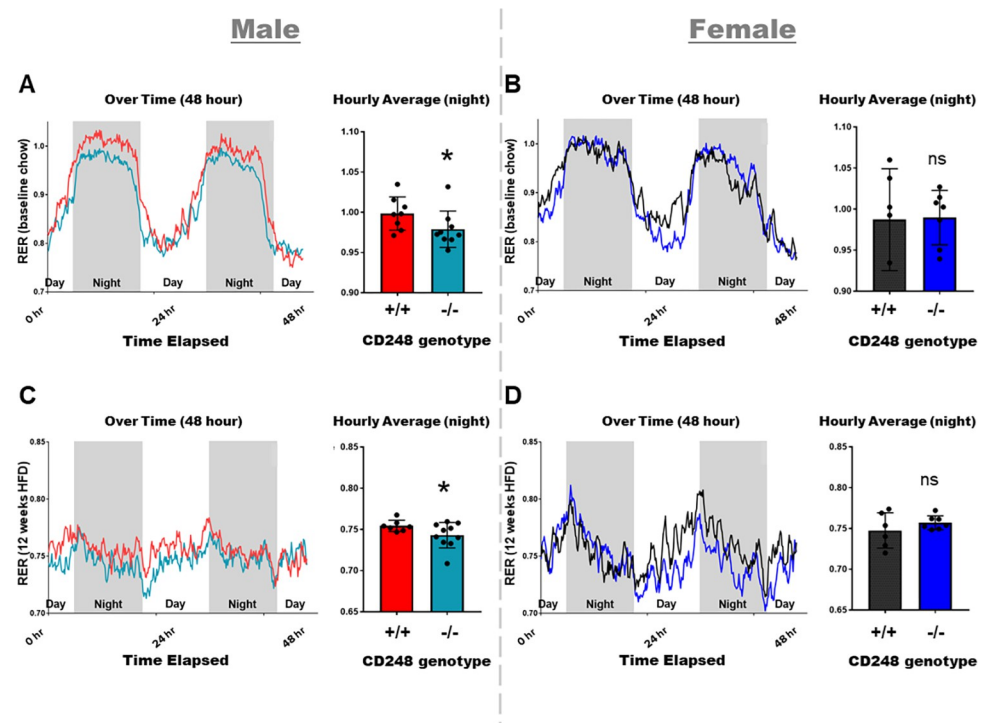


**Fig 2.** Respiratory exchange ratio (RER) as calculated from indirect calorimetry measurements over 48 hours: Chow-fed (A) males and (B) females; HFD-fed (C) males and (D) females. Line graphs indicate hourly averages over time whilst bar graphs show overall averages at night  $\pm$  SD. Body weight data over time were analysed for significant differences by t-test. RER data were analysed for significance by ANCOVA test to determine if the body weight covariable is responsible for the significant changes in RER. In all graphs: Cd248<sup>+/+</sup> males (red), Cd248<sup>-/-</sup> males (cyan), Cd248<sup>+/+</sup> females (black), Cd248<sup>-/-</sup> females (blue). Significant \*  $p \leq 0.05$ .

<https://doi.org/10.1371/journal.pone.0284012.g002>

high fat diet (Fig 2A & 2C), whilst no genotype-specific differences were detected between females (Fig 2B & 2D). A lower RER implies that the Cd248<sup>-/-</sup> male mice were oxidising more lipids than their wildtype littermates.

As Cd248 has been associated with inflammatory states in arthritis models [14], and given that inflammation can alter metabolic rate, one possibility behind the reduced weight gain was that it was due to an altered inflammatory state of the Cd248<sup>-/-</sup> males following 15 weeks HFD. Thus, quantification of 36 cytokines and chemokines (Luminex) known to be involved with inflammation was performed in the serum of the mice following 15 weeks of high fat diet (S1 Fig). No differences in these markers of inflammation were identified between Cd248<sup>+/+</sup> and Cd248<sup>-/-</sup> in either sex. To assess whether loss of Cd248 was protective against metabolic syndrome, glucose tolerance tests (GTT) were carried out at baseline (age 6–8 weeks), and 6 weeks, 12 weeks, and 15 weeks of high fat diet-feeding. Despite reduced weight gain, Cd248<sup>-/-</sup> males showed no difference in their response to GTT at any of the timepoints measured (Fig 3A, 3C and 3E). Females also showed no difference (Fig 3B, 3D and 3F). The reduced weight gain observed led us to hypothesise that male Cd248<sup>-/-</sup> mice had higher levels of adipocyte browning. To test this hypothesis, mice were stimulated with the  $\beta$ -adrenergic agonist CL316,243 whilst VO<sub>2</sub> was recorded in the PhenoMaster system. No significant differences were found. (Fig 3G & 3H).

Following 16 weeks of high fat diet-feeding, fat depots were assessed by mass spectrometry (by LC/MS) and gene expression analysis (Fig 4). Cd248 gene expression was detected at similar levels in the fat pads of wildtype animals, regardless of sex and was undetectable in all

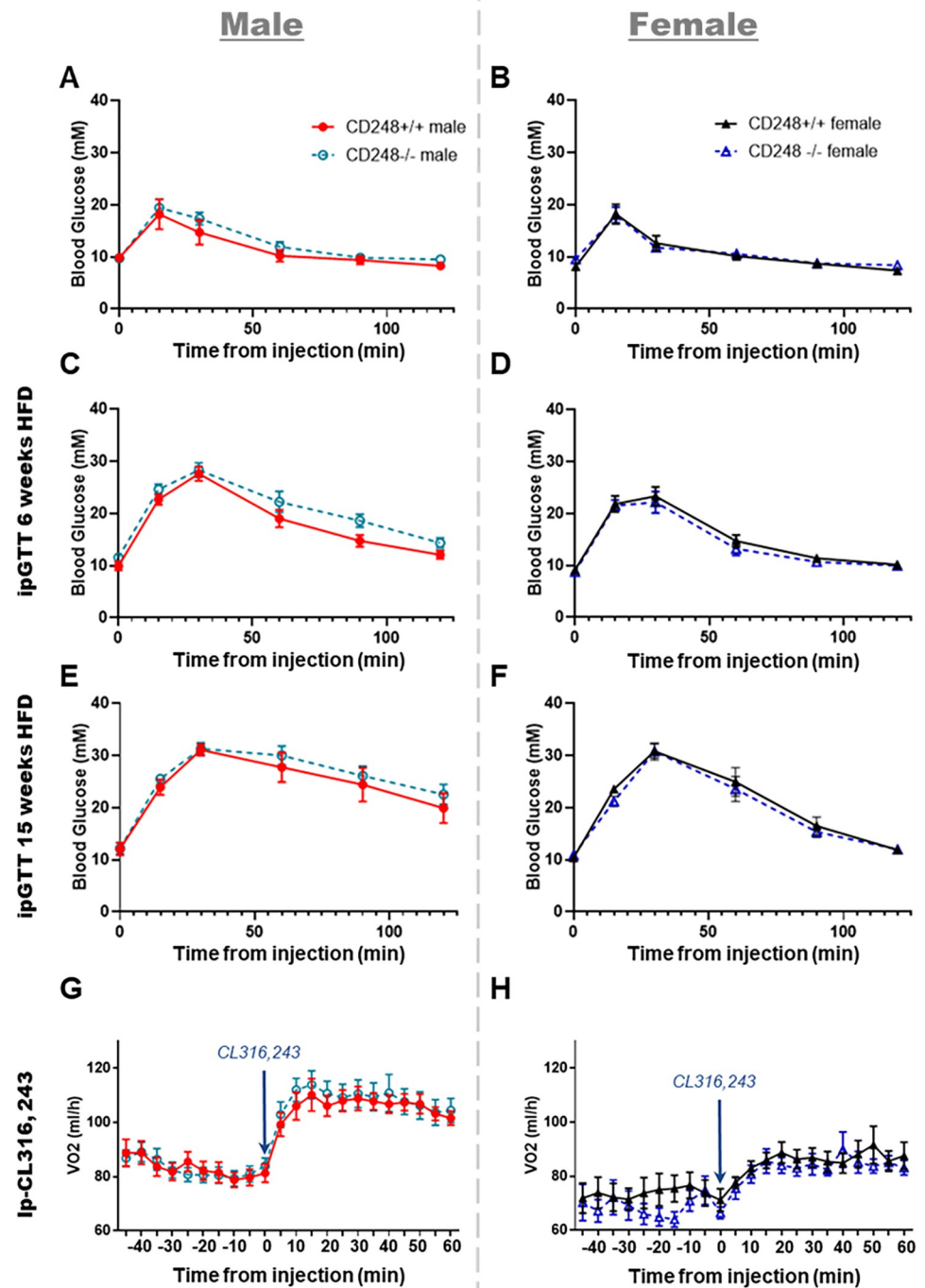


**Fig 3.** Glucose tolerance test (GTT) was performed at baseline in (A) males and (B) females (6–8 weeks old mice) and following high fat diet-feeding for 6 weeks (C) males and (D) females, then 15 weeks (E) males and (F) females. Response to CL316,243 injection was measured as average VO<sub>2</sub> over time in (G) males and (H) females. In all graphs: Cd248<sup>+/+</sup> males (red), Cd248<sup>-/-</sup> males (cyan), Cd248<sup>+/+</sup> females (black), Cd248<sup>-/-</sup> females (blue). Data were analysed for significant differences by ANOVA. No significant differences were found. All error bars  $\pm$  SEM.

<https://doi.org/10.1371/journal.pone.0284012.g003>

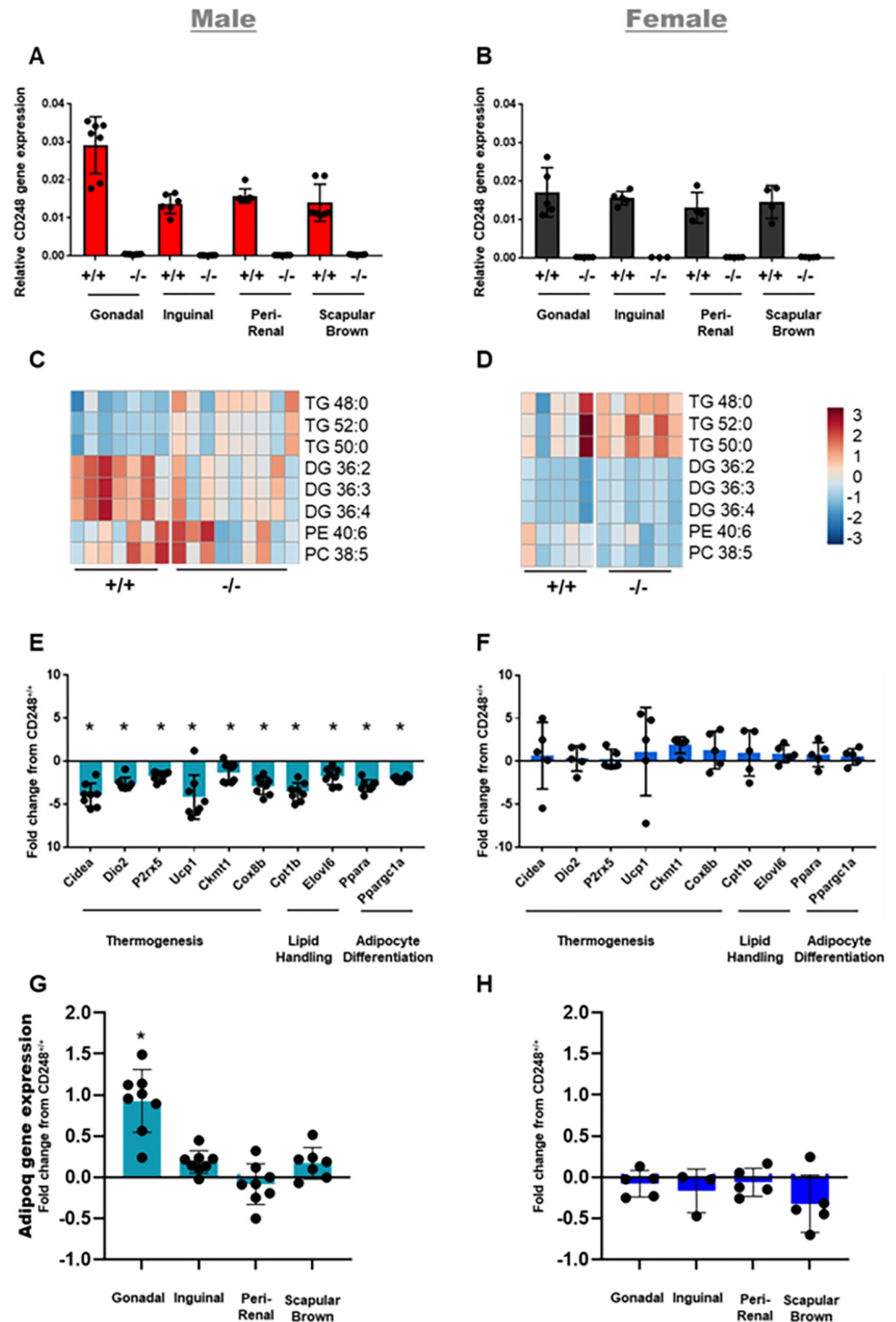


**Fig 4. Gene expression and lipidomic results from fat pads following high fat diet feeding for 16 weeks.** CD248 expression analysis in each fat pad confirmed loss of CD248 in  $Cd248^{-/-}$  tissues from (A) males (B) females. Heatmap showing z-scores (scale bar from blue = -3 to red = +3 shown—far right) of significantly altered lipids in (C) male  $Cd248^{-/-}$  perirenal fat pad compared to  $Cd248^{+/+}$  with (D) female shown for comparison where no significant differences were detected. Lipid notation follows the nomenclature described in Liebsch *et al.* 2013 [22]. Detail of the MSI identification level for each of the lipid species is given in S1 Table. Gene expression array showing significantly altered genes from (E) male  $Cd248^{-/-}$  perirenal fat pad, with (F) female shown for comparison where no significant differences were detected. Adipoq expression data for all four fat depots in (G) male and (H) female mice are also

shown. Results analysed for significant differences by t-test. Considered significant (\*) if t-test yielded  $p \leq 0.05$  and fold change or z score from control  $\geq 1.5$ . All error bars  $\pm$  SD.

<https://doi.org/10.1371/journal.pone.0284012.g004>

adipose tissues from *Cd248*<sup>-/-</sup> animals (Fig 4A and 4B). Lipidomic analysis of the scapular BAT, inguinal WAT, gonadal WAT and perirenal WAT identified sex-specific differences in lipid classes (S2 Fig): In the perirenal pads, *Cd248*<sup>-/-</sup> males had lower amounts of diglycerides compared to *Cd248*<sup>+/+</sup> males (Fig 4C). No significant differences were observed in fat pads from female mice (Fig 4D). RNA expression analysis was performed using a custom chip of 56 Taqman gene expression assays (comprising 52 target genes and 4 reference/housekeeping genes) against adipocyte associated genes, chosen to cover a range of different pathways and processes including adipocyte browning, lipid storage, mitochondrial function, and lipid metabolism. This analysis also identified sex-specific and depot-specific gene expression changes in male, but not female mice; notably the perirenal WAT of male *Cd248*<sup>-/-</sup> mice showed reduced expression of 10 genes involved in thermogenesis (*Cidea*, *P2rx5*, *Cox8b*, *Ckmt2*, *UCP1*, *Dio2*), lipid handling (*Cpt1b*, *Elovl6*) or adipocyte differentiation (*Ppara*, *Ppargc1a*) relative to *Cd248*<sup>+/+</sup> controls (Fig 4E), whilst *Adipoq* gene expression was increased in the gonadal fat pad only (Fig 4G). These changes were not identified in female mice (Fig 4F and 4H). Inguinal and scapular fat pads showed fewer differences compared to perirenal and gonadal fat pads (S3 Fig) indicating that visceral adipose tissue depots were most affected by genetic deletion of *Cd248*.

Given the altered weight gain and energy metabolism in *Cd248*<sup>-/-</sup> males, alongside the differences in lipid profile and gene expression in *Cd248*<sup>-/-</sup> male adipose tissue, we hypothesised that altered metabolic pathway(s) were intrinsic to *Cd248*<sup>-/-</sup> male adipocytes. To test this hypothesis, we performed metabolomic analysis by LC-MS on primary cultured differentiated preadipocytes extracted from the inguinal fat pad of male and female *Cd248*<sup>+/+</sup> and *Cd248*<sup>-/-</sup> mice (Fig 5). Analysis was performed on cells cultured under normal (10% FBS) serum conditions (Fig 5A and 5B) and following 2 hours serum starvation (Fig 5C and 5D). Several metabolites were found to be significantly different between *Cd248*<sup>+/+</sup> and *Cd248*<sup>-/-</sup>. Including those involved in vitamin B6 metabolism (pyridoxal, pyridoxalacetone, pyridoxate) or glutamine metabolism (glutarate, glutamate). More acute differences were observed between *Cd248*<sup>+/+</sup> and *Cd248*<sup>-/-</sup> in the male derived cells under serum starvation compared to the female. Expression of adipocyte differentiation marker, CD36 was equivalent across cells differentiated from all sexes and genotypes (Fig 5E and 5F).

## Discussion

The reduced weight gain phenotype seen in *Cd248*<sup>-/-</sup> males fed a high fat diet, whilst relatively mild, is consistent and robust, having been previously reported by a separate research group using a *Cd248*<sup>-/-</sup> mouse on a different background strain [11]. No such differences were seen in weight gain for *Cd248*<sup>-/-</sup> fed a chow diet [16]. Additionally, no differences were identified in circulating lipid levels or lipid accumulation in *Cd248*<sup>-/-</sup> mice fed chow diet, whilst these were identified on HFD [16]. These previous findings suggest that HFD stress is required to induce a metabolic syndrome phenotype in the absence of *Cd248*. Petrus et al (2019) also reported protection from glucose intolerance in *Cd248*<sup>-/-</sup> fed a high fat diet, however, this phenotype was not replicated in our study [11]. This disparity could be due to the variance in mouse strain or another difference in animal housing or conditions of which we are not aware. Indeed, mouse strain and sex are critical variables to consider in the interpretation of metabolic phenotypes identified from genetically modified mice. Ingvorsen et al (2017) previously assessed the effect of sex on response to HFD in a large sample-set (N = 659 female, 660 male)

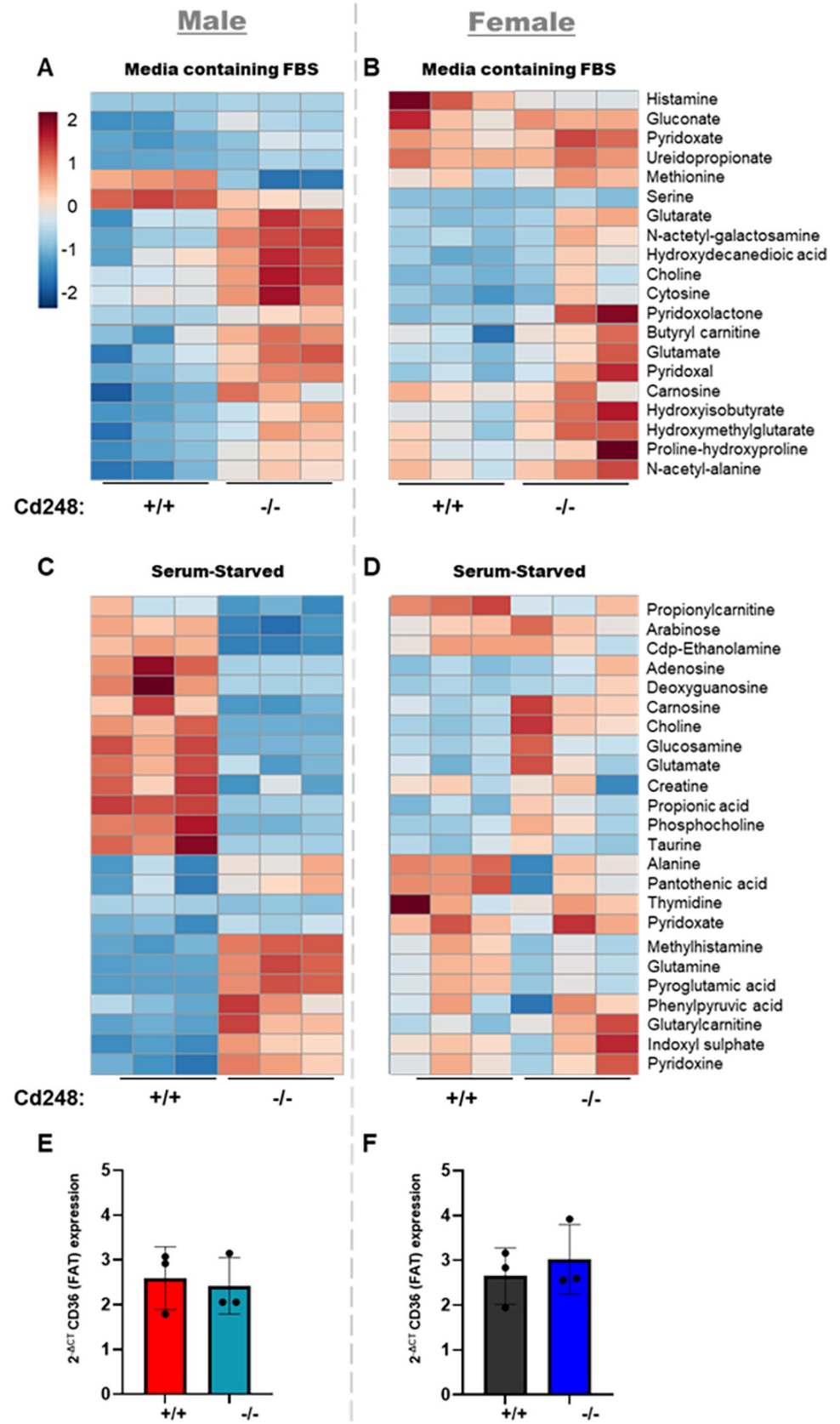


**Fig 5. Results from differentiated preadipocytes.** Heat map showing z-scores for metabolites identified as significantly altered in cells isolated from male mice. *Cd248*<sup>+/+</sup> and *Cd248*<sup>-/-</sup> differentiated preadipocytes from chow fed (A) males and (B) females were cultured in 10% FBS media (Media containing FBS) or following 2 hours of serum starved conditions: (C) males and (D) females. Scale bar from blue = -2 to red = +2 (shown top left). Analysis for significant differences by t-test. Considered significant if t-test yielded  $p \leq 0.05$  and z-score from control  $\geq 1.5$ . Detail of the MSI identification level for each of the metabolite species is given in S2 and S3 Tables for culture in media containing FBS and serum starved conditions, respectively. Expression levels of adipocyte differentiation marker, CD36 (normalised to housekeeping gene) are shown for (E) male and (F) female-derived cells. No significant difference was detected.

<https://doi.org/10.1371/journal.pone.0284012.g005>

of C57BL/6N mice, and demonstrated that male mice are more sensitive to high-fat diet-induced obesity and to glucometabolic changes than female mice of the same strain [23]. In another large study (>300 mice), Wang et al (2006) explored the influence of sex on inheritance of quantitative trait loci (QTL) and their subsequent influence on obesity in the APOE knockout mouse, a strain used widely in obesity and metabolic syndrome studies [8]. They identified a “remarkably high degree of sex-dependence on both the cis and trans regulation of gene expression” [8]. We have controlled against the risk of genetic drift by comparing mice from cohorts of heterozygous pairings to ensure analysis of littermate controls throughout this study. Expression of CD248 between male and female wildtype mice is equivalent in all fat pads except the gonadal, where expression is higher in males. Given that significant differences in genes involved in thermogenesis, lipid handling and adipocyte differentiation were seen only in the male perirenal fat pad, we do not conclude that sex differences in CD248 gene expression are the primary cause of this phenotype.

By performing experiments on male and female wildtype mice in parallel, we can see that female mice showed a metabolic response to HFD in this study, as seen by alterations in RER and glucose tolerance, although weight gain was more variable in the female cohort.

To understand the cause of the reduced weight gain identified specifically in male *Cd248*<sup>-/-</sup> mice, we performed indirect calorimetry, which identified a lower RER in *Cd248*<sup>-/-</sup> males relative to littermate *Cd248*<sup>+/+</sup>, indicative of increased lipid oxidation. We investigated whether the reduced weight gain in *Cd248*<sup>-/-</sup> males was due to either inflammation or adipocyte browning. However, we found no differences in inflammatory cytokines in the serum of *Cd248*<sup>-/-</sup> mice on high fat diet. We also found no difference in expression of adipocyte browning-associated genes and no difference in the response to beta-adrenergic stimulation between *Cd248*<sup>-/-</sup> mice and littermate controls. These data do not suggest that an underlying pro-inflammatory or adipocyte browning phenotype is the primary cause of the increased lipid oxidation. Of note, there is a lack of consensus in the published data concerning the gene and protein expression of CD248 in brown adipose tissue. Here, in the mouse, we detected similar levels of mRNA in white (gonadal, inguinal, and peri-renal) depots as compared to scapular brown fat, confirming the findings of Roh et al. (2018) but at odds with those of Petrus et al. (2019) who did not detect Cd248 in BAT [11, 24]. At the protein level, Muller et al. (2016) identified CD248 in human BAT whilst Li et al. (2020) did not detect it in murine BAT [25, 26]. The phenotypes we have detected in the *Cd248*<sup>-/-</sup> mouse are all seen in the WAT compartment, where Cd248 expression is not disputed, however we highlight this uncertainty to the reader for completeness and consideration when interpreting the findings.

Lipidomics uncovered a difference in lipid profile in the male *Cd248*<sup>-/-</sup> perirenal fat pad. Diglycerides alongside phosphatidylethanolamine and phosphocholine were found to be altered. This observation is noteworthy as these lipid species are utilised in synthesis of the cell membrane, and this corroborates the possible differences in the Lands Cycle observed by us previously in plasma [16]. Differences in the lipids detected in fat pads imply that *Cd248* has a role in localised fat deposition. Although the mechanism behind this is unclear, it is supported

by gene expression changes observed in specific fat depots. In perirenal WAT, we find lower expression of transporter *Cpt1b*, which imports fatty acids to mitochondria [27]; reduced expression of enzyme *Elovl6*, which is required for fatty acid polymerisation [28, 29]; lower levels of *Cidea*, a transcription factor known to regulate lipolysis and energy expenditure [30] and downregulation of *Dio2*, which is associated with adipocyte browning [31] and has also shown a sex-specific phenotype [32]. Downregulation of *Ppara* was also observed in *Cd248*<sup>-/-</sup> mice, which is a known regulator of adipocyte differentiation and lipid metabolism [33]. In gonadal WAT there is significantly higher expression of the adipokine Adiponectin (Adipoq), which is known to promote fatty acid oxidation and impair adipocyte differentiation in mice [34, 35].

The metabolites found to be altered by LC-MS include those involved in vitamin B6 metabolism (pyridoxal, pyridoxalacetone, pyridoxate). Vitamin B6 has been associated with lipid deposition since the 1970s [36] and more recently expression of a kinase in this pathway was found to control adipogenesis and insulin signalling [37]. Metabolites from glutamate metabolism are also altered (glutarate, glutamate, glutamine). Glutamine has recently been demonstrated to correlate with inflammation of adipose tissue in obesity [38]. Glutaryl carnitine was found to be elevated in cells derived from male *Cd248*<sup>-/-</sup> mice, when cultured in the absence of serum, whilst O-acetylcarnitine was found to be elevated in normal conditions. These findings correlate with the observation that expression of *Cpt1b* was downregulated in male *Cd248*<sup>-/-</sup> adipose tissue, given that this transporter is required for uptake of carnitines into mitochondria for beta-oxidation.

The differences identified in cells and tissues from male *Cd248*<sup>-/-</sup> mice were not evident in female mice. Similarly, no phenotypic differences were observed in female *Cd248*<sup>-/-</sup> compared to their *Cd248*<sup>+/+</sup> littermates. These experimental results demonstrate a sex-specific role for *Cd248* in lipid deposition in mice, adding to the body of knowledge of sex differences in adipose tissue metabolism. We cannot exclude the influence of sex hormones (including their potentially long-lasting effects in our primary cell culture findings) or the potential role of sex-linked inheritance of CD248-interacting genes in the causation of the male-specific phenotype observed on genetic deletion of CD248. Petrus et al (2019) previously demonstrated a reduction in CD248 expression in human females following post-bariatric surgery [11]. Whilst a similar male cohort was not available for comparison in this case, and correlation does not necessarily imply causation, these results, in the light of our findings, reinforce the importance of using both sexes in metabolic studies and the potential for key differences between model species and human disease. Indeed, increasing appreciation of the importance of sexual dimorphism has led the United States National Institutes of Health (NIH) and the UK governmental funding agency (UKRI) (in 2016 and 2022, respectively) to direct researchers to avoid sex-bias in study design [39–41]. Given the great scientific effort spent on understanding the mechanisms behind adipogenesis, lipogenesis and adipocyte browning and the wide usage of murine models to understand these processes, our data demonstrate the importance of performing such studies on both sexes, both *in vitro* and *in vivo*.

## Supporting information

**S1 Fig. Selected Luminex panel results pg/ml ± SD.** Serum collected at end of high fat diet study resulted in 6x *Cd248*<sup>+/+</sup> male, 7x *Cd248*<sup>-/-</sup> male, 5x *Cd248*<sup>+/+</sup> female and 6x *Cd248*<sup>-/-</sup> female. Results analysed for significant differences by t test. No significant differences found in either male or female serum.

(TIF)

**S2 Fig. Lipidomics results for each fat pad.** Differences in certain classes of triglycerides (TGs), diglycerides (DGs) alongside Phosphatidylethanolamine (PE) and phosphocholine

(PC) are found. (A) Heatmap of Cd248<sup>+/+</sup> compared to Cd248<sup>-/-</sup>, showing differences in lipid classes from male brown adipose tissue. (B) Heat map of Cd248<sup>+/+</sup> and Cd248<sup>-/-</sup> showing differences in lipid classes from female brown adipose tissue. (C) Heat map of Cd248<sup>+/+</sup> and Cd248<sup>-/-</sup>, showing differences in lipid classes from male inguinal adipose tissue. (D) Heat map of Cd248<sup>+/+</sup> and Cd248<sup>-/-</sup>, showing differences in lipid classes from female inguinal adipose tissue. (E) Heat map of Cd248<sup>+/+</sup> and Cd248<sup>-/-</sup>, showing differences in lipid classes from male gonadal adipose tissue. (F) Heat map of Cd248<sup>+/+</sup> and Cd248<sup>-/-</sup>, showing differences in lipid classes from female gonadal adipose tissue. Scale bar from blue = -4 to red = +4 is shown on top left. Lipid notation follows the nomenclature described in Liebisch *et al.* 2013 [22].

(TIF)

**S3 Fig. Gene expression results each fat pad.** These ten genes were found to be significantly altered in the male perirenal fat pad. Their expression in the other fat pads isolated is included here for comparison. No significant differences were observed. Bar graphs showing fold change in expression of ten genes (x axis) in Cd248<sup>-/-</sup> compared to Cd248<sup>+/+</sup> mice fat depots: (A) male BAT; (B) Female BAT; (C) Male ingWAT; (D) Female ingWAT; (E) Male gonWAT and (F) Female gonWAT.

(TIF)

**S1 Table. Lipid information for Fig 4C and 4D.**

(DOCX)

**S2 Table. Metabolite information for Fig 5A and 5B.**

(DOCX)

**S3 Table. Metabolites information for Fig 5C and 5D.**

(DOCX)

**S4 Table. The number of detected metabolites and lipids.**

(DOCX)

**S5 Table. OpenArray and Luminex gene/protein list.**

(DOCX)

## Author Contributions

**Conceptualization:** David Baker, Christopher Church, Graeme Davies, Gareth Lavery, Amy J. Naylor.

**Data curation:** Kieran Patrick, Xiang Tian.

**Formal analysis:** Kieran Patrick, Xiang Tian.

**Funding acquisition:** Amy J. Naylor.

**Investigation:** Kieran Patrick, Xiang Tian, David Cartwright, Silke Heising, Matthew S. Glover, Ellie N. Northall, Graeme Davies.

**Project administration:** Amy J. Naylor.

**Resources:** Lisa Cazares, Sonja Hess, David Baker, Gareth Lavery.

**Supervision:** Lisa Cazares, Sonja Hess, Christopher Church, Graeme Davies, Gareth Lavery, Amy J. Naylor.

**Writing – original draft:** Kieran Patrick, Graeme Davies, Amy J. Naylor.



**Writing – review & editing:** Kieran Patrick, Xiang Tian, David Cartwright, Silke Heising, Matthew S. Glover, Lisa Cazares, Sonja Hess, David Baker, Christopher Church, Gareth Lavery, Amy J. Naylor.

## References

1. Zwick RK, Guerrero-Juarez CF, Horsley V, Plikus M V. Anatomical, Physiological, and Functional Diversity of Adipose Tissue. *Cell Metab*. 2018; 27: 68–83. <https://doi.org/10.1016/j.cmet.2017.12.002> PMID: 29320711
2. Yang C-F, Liu W-W, Wang H-Q, Zhang J-L, Li K, Diao Z-Y, et al. Gonadal white adipose tissue is important for gametogenesis in mice through maintenance of local metabolic and immune niches. *Journal of Biological Chemistry*. 2022; 298: 101818. <https://doi.org/10.1016/j.jbc.2022.101818> PMID: 35278432
3. van Beek L, van Klinken JB, Pronk ACM, van Dam AD, Dirven E, Rensen PCN, et al. The limited storage capacity of gonadal adipose tissue directs the development of metabolic disorders in male C57Bl/6J mice. *Diabetologia*. 2015; 58: 1601–1609. <https://doi.org/10.1007/s00125-015-3594-8> PMID: 25962520
4. Tramunt B, Smati S, Grandgeorge N, Lenfant F, Arnal J-F, Montagner A, et al. Sex differences in metabolic regulation and diabetes susceptibility. *Diabetologia*. 2020; 63: 453–461. <https://doi.org/10.1007/s00125-019-05040-3> PMID: 31754750
5. Bi Y, Jiang M, Guo W, Guan X, Xu M, Ren S, et al. Sex-Dimorphic and Sex Hormone-Dependent Role of Steroid Sulfatase in Adipose Inflammation and Energy Homeostasis. *Endocrinology*. 2018; 159: 3365–3377. <https://doi.org/10.1210/en.2018-00531> PMID: 30060148
6. Bjorntorp P. Hormonal control of regional fat distribution. *Human Reproduction*. 1997; 12: 21–25. [https://doi.org/10.1093/humrep/12.suppl\\_1.21](https://doi.org/10.1093/humrep/12.suppl_1.21) PMID: 9403318
7. Sebo ZL, Rodeheffer MS. Prepubertal androgen signaling is required to establish male fat distribution. *Stem Cell Reports*. 2022; 17: 1081–1088. <https://doi.org/10.1016/j.stemcr.2022.04.001> PMID: 35487210
8. Wang S, Yehya N, Schadt EE, Wang H, Drake TA, Lusis AJ. Genetic and Genomic Analysis of a Fat Mass Trait with Complex Inheritance Reveals Marked Sex Specificity. *PLoS Genet*. 2006; 2: e15. <https://doi.org/10.1371/journal.pgen.0020015> PMID: 16462940
9. Naylor AJ, Azzam E, Smith S, Croft A, Poyser C, Duffield JS, et al. The mesenchymal stem cell marker CD248 (endosialin) is a negative regulator of bone formation in mice. *Arthritis Rheum*. 2012; 64: 3334–3343. <https://doi.org/10.1002/art.34556> PMID: 22674221
10. MacFadyen JR, Haworth O, Roberston D, Hardie D, Webster M-T, Morris HR, et al. Endosialin (TEM1, CD248) is a marker of stromal fibroblasts and is not selectively expressed on tumour endothelium. *FEBS Lett*. 2005; 579: 2569–2575. <https://doi.org/10.1016/j.febslet.2005.03.071> PMID: 15862292
11. Petrus P, Fernandez TL, Kwon MM, Huang JL, Lei V, Safikhani NS, et al. Specific loss of adipocyte CD248 improves metabolic health via reduced white adipose tissue hypoxia, fibrosis and inflammation. *EBioMedicine*. 2019; 44: 489–501. <https://doi.org/10.1016/j.ebiom.2019.05.057> PMID: 31221584
12. Xu C, Zhang K, Yang F, Zhou X, Liu S, Li Y, et al. CD248+ Cancer-Associated Fibroblasts: A Novel Prognostic and Therapeutic Target for Renal Cell Carcinoma. *Front Oncol*. 2021; 11. <https://doi.org/10.3389/fonc.2021.773063> PMID: 34970489
13. Smith SW, Eardley KS, Croft AP, Nwosu J, Howie AJ, Cockwell P, et al. CD248+ stromal cells are associated with progressive chronic kidney disease. *Kidney Int*. 2011; 80: 199–207. <https://doi.org/10.1038/ki.2011.103> PMID: 21490589
14. Maia M, de Vriese A, Janssens T, Moons M, van Landuyt K, Tavernier J, et al. CD248 and its cytoplasmic domain: A therapeutic target for arthritis. *Arthritis Rheum*. 2010; 62: 3595–3606. <https://doi.org/10.1002/art.27701> PMID: 20722022
15. Hasanov Z, Ruckdeschel T, König C, Mogler C, Kapel SS, Korn C, et al. Endosialin Promotes Atherosclerosis Through Phenotypic Remodeling of Vascular Smooth Muscle Cells. *Arterioscler Thromb Vasc Biol*. 2017; 37: 495–505. <https://doi.org/10.1161/ATVBAHA.116.308455> PMID: 28126825
16. Armitage EG, Barnes A, Patrick K, Bechar J, Harrison MJ, Lavery GG, et al. Metabolic consequences for mice lacking Endosialin: LC-MS/MS-based metabolic phenotyping of serum from C56Bl/6J Control and CD248 knock-out mice. *Metabolomics*. 2021; 17: 14. <https://doi.org/10.1007/s11306-020-01764-1> PMID: 33462674
17. Kilkenny C, Browne WJ, Cuthill IC, Emerson M, Altman DG. Improving Bioscience Research Reporting: The ARRIVE Guidelines for Reporting Animal Research. *PLoS Biol*. 2010; 8: e1000412. <https://doi.org/10.1371/journal.pbio.1000412> PMID: 20613859

18. Nanda A, Karim B, Peng Z, Liu G, Qiu W, Gan C, et al. Tumor endothelial marker 1 (Tem1) functions in the growth and progression of abdominal tumors. *Proceedings of the National Academy of Sciences*. 2006; 103: 3351–3356. <https://doi.org/10.1073/pnas.0511306103> PMID: 16492758
19. Cartwright DM, Oakey LA, Fletcher RS, Doig CL, Heising S, Larner DP, et al. Nicotinamide riboside has minimal impact on energy metabolism in mouse models of mild obesity. *Journal of Endocrinology*. 2021; 251: 111–123. <https://doi.org/10.1530/JOE-21-0123> PMID: 34370682
20. Sangster T, Major H, Plumb R, Wilson AJ, Wilson ID. A pragmatic and readily implemented quality control strategy for HPLC-MS and GC-MS-based metabolomic analysis. *Analyst*. 2006; 131: 1075. <https://doi.org/10.1039/b604498k> PMID: 17003852
21. Sumner LW, Amberg A, Barrett D, Beale MH, Beger R, Daykin CA, et al. Proposed minimum reporting standards for chemical analysis. *Metabolomics*. 2007; 3: 211–221. <https://doi.org/10.1007/s11306-007-0082-2> PMID: 24039616
22. Liebisch G, Vizcaino JA, Köfeler H, Trötzmüller M, Griffiths WJ, Schmitz G, et al. Shorthand notation for lipid structures derived from mass spectrometry. *J Lipid Res*. 2013; 54: 1523–1530. <https://doi.org/10.1194/jlr.M033506> PMID: 23549332
23. Ingvorsen C, Karp NA, Lelliott CJ. The role of sex and body weight on the metabolic effects of high-fat diet in C57BL/6N mice. *Nutr Diabetes*. 2017; 7: e261–e261. <https://doi.org/10.1038/nutd.2017.6> PMID: 28394359
24. Roh HC, Tsai LTY, Shao M, Tenen D, Shen Y, Kumari M, et al. Warming Induces Significant Reprogramming of Beige, but Not Brown, Adipocyte Cellular Identity. *Cell Metab*. 2018; 27: 1121–1137.e5. <https://doi.org/10.1016/j.cmet.2018.03.005> PMID: 29657031
25. Müller S, Balaz M, Stefanicka P, Varga L, Amri E-Z, Ukropec J, et al. Proteomic Analysis of Human Brown Adipose Tissue Reveals Utilization of Coupled and Uncoupled Energy Expenditure Pathways. *Sci Rep*. 2016; 6: 30030. <https://doi.org/10.1038/srep30030> PMID: 27418403
26. Li J, Li J, Zhao W-G, Sun H-D, Guo Z-G, Liu X-Y, et al. Comprehensive proteomics and functional annotation of mouse brown adipose tissue. *PLoS One*. 2020; 15: e0232084. <https://doi.org/10.1371/journal.pone.0232084> PMID: 32374735
27. Kim T. Carnitine Palmitoyltransferase 1b Deficient Mice Develop Severe Insulin Resistance After Prolonged High Fat Diet Feeding. *J Diabetes Metab*. 2014;05. <https://doi.org/10.4172/2155-6156.1000401> PMID: 25580367
28. Tan CY, Virtue S, Bidault G, Dale M, Hagen R, Griffin JL, et al. Brown Adipose Tissue Thermogenic Capacity Is Regulated by Elovl6. *Cell Rep*. 2015; 13: 2039–2047. <https://doi.org/10.1016/j.celrep.2015.11.004> PMID: 26628376
29. Moon Y-A, Ochoa CR, Mitsche MA, Hammer RE, Horton JD. Deletion of ELOVL6 blocks the synthesis of oleic acid but does not prevent the development of fatty liver or insulin resistance. *J Lipid Res*. 2014; 55: 2597–2605. <https://doi.org/10.1194/jlr.M054353> PMID: 25281760
30. Zhou Z, Yon Toh S, Chen Z, Guo K, Peng Ng C, Ponniah S, et al. Cidea-deficient mice have lean phenotype and are resistant to obesity. *Nat Genet*. 2003; 35: 49–56. <https://doi.org/10.1038/ng1225> PMID: 12910269
31. Christoffolete MA, Linardi CCG, de Jesus L, Ebina KN, Carvalho SD, Ribeiro MO, et al. Mice with Targeted Disruption of the Dio2 Gene Have Cold-Induced Overexpression of the Uncoupling Protein 1 Gene but Fail to Increase Brown Adipose Tissue Lipogenesis and Adaptive Thermogenesis. *Diabetes*. 2004; 53: 577–584. <https://doi.org/10.2337/diabetes.53.3.577> PMID: 14988240
32. Carmody C, Ogawa-Wong AN, Martin C, Luongo C, Zuidwijk M, Sager B, et al. A Global Loss of Dio2 Leads to Unexpected Changes in Function and Fiber Types of Slow Skeletal Muscle in Male Mice. *Endocrinology*. 2019; 160: 1205–1222. <https://doi.org/10.1210/en.2019-00088> PMID: 30951174
33. Howroyd P, Swanson C, Dunn C, Cattley RC, Corton JC. Decreased Longevity and Enhancement of Age-Dependent Lesions in Mice Lacking the Nuclear Receptor Peroxisome Proliferator-Activated Receptor  $\alpha$  (PPAR $\alpha$ ). *Toxicol Pathol*. 2004; 32: 591–599. <https://doi.org/10.1080/01926230490515283> PMID: 15603543
34. Fruebis J. Proteolytic cleavage product of 30-kDa adipocyte complement-related protein increases fatty acid oxidation in muscle and causes weight loss in mice. *Proceedings of the National Academy of Sciences*. 2001; 98: 2005–2010. <https://doi.org/10.1073/pnas.98.4.2005> PMID: 11172066
35. Bauche IB, El Mkaem SA, Pottier A-M, Senou M, Many M-C, Rezsohazy R, et al. Overexpression of Adiponectin Targeted to Adipose Tissue in Transgenic Mice: Impaired Adipocyte Differentiation. *Endocrinology*. 2007; 148: 1539–1549. <https://doi.org/10.1210/en.2006-0838> PMID: 17204560
36. Lemonnier D, de Gasquet P, Griglio S, Naon R, Reynouard F, Trémoilières J. Effect of Dietary Vitamin B Level on Fat Storage, Adipose Tissue Cellularity and Energy Expenditure in Rats and Mice Fed a High-Fat Diet. *Ann Nutr Metab*. 1974; 16: 15–29. <https://doi.org/10.1159/000175469> PMID: 4836680

37. Martínez-Sánchez N, Moreno-Navarrete JM, Contreras C, Rial-Pensado E, Fernø J, Nogueiras R, et al. Thyroid hormones induce browning of white fat. *Journal of Endocrinology*. 2017; 232: 351–362. <https://doi.org/10.1530/JOE-16-0425> PMID: 27913573
38. Petrus P, Lecoutre S, Dollet L, Wiel C, Sulen A, Gao H, et al. Glutamine Links Obesity to Inflammation in Human White Adipose Tissue. *Cell Metab*. 2020; 31: 375–390.e11. <https://doi.org/10.1016/j.cmet.2019.11.019> PMID: 31866443
39. Arnegard ME, Whitten LA, Hunter C, Clayton JA. Sex as a Biological Variable: A 5-Year Progress Report and Call to Action. *J Womens Health*. 2020; 29: 858–864. <https://doi.org/10.1089/jwh.2019.8247> PMID: 31971851
40. Miller LR, Marks C, Becker JB, Hurn PD, Chen W, Woodruff T, et al. Considering sex as a biological variable in preclinical research. *The FASEB Journal*. 2017; 31: 29–34. <https://doi.org/10.1096/fj.201600781R> PMID: 27682203
41. Karp NA, Reavey N. Sex bias in preclinical research and an exploration of how to change the status quo. *Br J Pharmacol*. 2019; 176: 4107–4118. <https://doi.org/10.1111/bph.14539> PMID: 30418665